Multi-Objective Stochastic Economic Dispatch with Maximal Renewable Penetration under Renewable Obligation

Thabo G. Hlalele[a,*], Raj M. Naidoo[a], Ramesh C. Bansal[b], Jiangfeng Zhang[c]

[a] *Department of Electrical, Electronic and Computer Engineering, University of Pretoria, Pretoria 0002, South Africa.*

[b] *Department of Electrical Engineering, University of Sharjah, Sharjah, United Arab Emirates.*

[c] *Department of Automotive Engineering, Clemson University, Greenville, SC 29607, US.*

Abstract

In this paper, a stochastic multi-objective economic dispatch model is presented under renewable obligation policy framework. This proposed model minimises the total operating costs of generators and spinning reserves under renewable obligation while maximising renewable penetration. The intermittent nature of the wind and photovoltaic power plants is incorporated into the renewable obligation model. In order to minimise the cycling costs associated with ramping the thermal generators, the battery energy storage system units are included in the model to assist the system spinning reserves. Dynamic scenarios are created to deal with the intermittency of renewable energy sources. Due to the computational complexity of all possible scenarios, a scenario reduction method is applied to reduce the number of scenarios and solve the proposed stochastic renewable obligation model. A Pareto optimal solution is presented for the renewable obligation, and further decision making is conducted to assess the trade-offs associated with the Pareto front. To show the effectiveness of the proposed stochastic renewable obligation model, two IEEE test systems are used, i.e., the modified IEEE 30-bus and IEEE 118-bus system. In both test systems, the proposed model can attain high renewable penetration while minimising the expected operating cost. In the large IEEE 118-bus test system, the computational efficiency

*Corresponding author.

Email address: greg.hlalele@gmail.com (Thabo G. Hlalele)

of the renewable obligation model is demonstrated by reducing the line constraints by 87% which minimises the computing time. A comparative study evaluates the impact of the stochastic model to the deterministic one, and it shows that the stochastic model can achieve high renewable penetration.

Keywords:
Battery energy storage system, Pareto frontier, photovoltaic generators, renewable energy obligation, stochastic dynamic economic dispatch, scenario generation, wind energy generators.

Nomenclature

Parameters

α	Renewable energy obligation requirement
η_c, η_d	BESS charging and discharging efficiency
γ	Renewable energy penalty cost in US dollars
π_ω	Probability of each scenario
ρ	Spinning reserve cost coefficient of the gth thermal generator in \$/MWh
τ	BESS energy cost in \$/MWh
φ	PV generator cost in \$/MWh
ζ	Wind generator cost in \$/MWh
C_g	Thermal generator g marginal cost
C_m	Wind generator m tariff cost
C_r	Thermal generator spinning reserve r operating cost
C_s	BESS generator s tariff cost
C_v	PV generator v tariff cost
DR_g	Ramp down limit for the gth thermal generator in MW/h

$E_{s,max}$	Maximum stored energy from s BESS generator in MWh
$E_{s,min}$	Minimum stored energy from s BESS generator in MWh
$P_{b,t}$	System demand at bus b, and time t in MW
$P_{g,max}$	Maximum output power from the gth thermal generator in MW
$P_{g,min}$	Minimum output power from the gth thermal generator in MW
$P_{l,t,\omega}$	Transmission line power flow at time t and scenario ω in MW
$P_{m,t,\omega}$	Output power from the mth wind farm at time t and scenario ω in MW
$P_{s,max}$	Maximum output power from the s BESS plant at time t and scenario ω in MW
$P_{v,t,\omega}$	Output power from the vth PV plant at time t and scenario ω in MW
$SRR_{r,max}$	Maximum spinning reserve requirement for the gth thermal generator in MW
UR_g	Ramp up limit for the gth thermal generator in MW/h

Indices and Sets

b	Index of buses
g	Index of thermal generators
l	Index of transmission lines
m	Index of wind generators
N_G	Set of thermal generators
N_L	Set of transmission lines
N_M	Set of wind generators

N_V	Set of photovoltaic generators
N_Ω	Set of scenarios and ω is the index of scenarios
N_B	Set of buses
N_R	Set of generator spinning reserves
N_S	Set of battery energy storage systems
r	Index of generator spinning reserves
s	Index of battery energy storage system
T	Time interval period
v	Index of photovoltaic generators

Variables

$P_{g,t,\omega}$	Scheduled output power for thermal generator g at time t in scenario ω
$P_{m,t,\omega}$	Scheduled output power for wind farm m at time t in scenario ω
$P_{r,t,\omega}$	Scheduled output power for thermal generator spinning reserve r at time t in scenario ω
$P_{s,t,\omega}$	Scheduled output power for BESS generator s at time t in scenario ω
$P^c_{s,t,\omega}$	BESS generator s charging mode at time t in scenario ω
$P^d_{s,t,\omega}$	BESS generator s discharge mode at time t in scenario ω
$P_{v,t,\omega}$	Scheduled output power for PV generator v at time t in scenario ω
$x_{s,t,\omega}$	Binary status of the BESS generator s discharging mode at time t in scenario ω
$y_{s,t,\omega}$	Binary status of the BESS generator s charging mode at time t in scenario ω

1. Introduction

The intermittent nature of renewable energy sources (RES) has created a challenge for their integration into the conventional power system. This increase in stochastic RES generators has escalated the cycling cost of thermal generators and has resulted in high operating costs. Consequently, it is very important to include the stochastic nature of wind and photovoltaic (PV) power plants to reduce uncertainty in generation scheduling and allow a smooth integration into the power system. As part of the integration of RES generators to the power system it is important to quantify the level of RES penetration to adequately operate the power system within its operational limits. A typical quantity based instrument used to quantify the level of RES penetration in the grid is known as a renewable obligation (RO). It refers to the minimum renewable energy quota to be adhered to without imposing any penalty for non-compliance. A useful tool used to quantify the dispatch of intermittent energy sources is the classic economic dispatch. Economic dispatch is a power system operation problem which optimises the generation resources within each dispatch interval.

In general, there are two policy frameworks that are commonly used to boost the penetration of RES [1]. A tariff-based instrument is the feed-in tariff (FIT), which provides an economic incentive for generating electricity using RES. A quantity-based instrument requires electricity suppliers to comply to a minimum renewable energy quota. This is known as RO in the UK or renewable purchase obligation (RPO) in other parts of the world. The RO allows electricity suppliers to buy a specified amount of their electricity sales from renewable sources. For each renewable energy sale, a renewable obligation certificate (ROC) is issued to demonstrate compliance to RES quota. Normally, a single ROC is equivalent to 1 MWh of renewable energy production. If the RES quota is not achieved, a penalty is payable by the generation companies. This approach of RO is used to support large scale generation of RES by fast tracking the integration of RES in the power system. This type of policy framework requires that a certain percentage of energy is attributed to RES and under this agreement a penalty is imposed for non-compliance. Moreover, the renewable energy quota is measured annually. This policy framework guarantees the use of renewables in the electricity generation as the RES target is dependent on the countries renewable energy policy and is administrated by the system operator (SO).

The increased level of RES penetration is normally approached from a dy-

namic economic dispatch (DED) point of view. In [2], [3], a DED with wind and PV injection is considered using the method of penalising the under and over estimation of the RES generators. The method used in approximating the under and over estimation of RES penetration considers the Weibull probability density function (PDF) for wind generation and a bi-modal Weibull or Beta PDF for PV generation. The conventional DED has made great strides in approximating the level of RES penetration in the grid. It, however, has a limitation since it does not include the uncertainty of renewable generation and system demand. This has led to two main approaches adopted by many researchers for including uncertainty which are robust optimisation and stochastic programming.

The addition of large-scale intermittent energy sources such PV and wind generators has adversely affected thermal generators performance in the power system. Their integration has increased the cycling costs of thermal generators [4]. This has led to an overall increase in maintenance cost of thermal generators [5]. To lower the variability and uncertainty of RES integration, both robust and stochastic optimisation framework are used for optimal scheduling of RES and thermal generators [6].

In the robust optimisation approach studied in [7], the aim is to scale down the ramping and cycling rates of thermal generators. This is performed to reduce the total operating costs associated with high RES penetration using a chance constraint approach. In [8], a DED problem with wind penetration is changed into a robust optimisation model and further transformed into a deterministic problem. The purpose of the model is to lessen the uncertainty of the wind power generation and improve the different levels of adjustable uncertainty budget. An adaptive robust optimisation is presented in [9], where a multi-period economic dispatch is used to model the uncertainty related to temporal and spatial correlations of wind power generators. In [10], [11] the stability of the power system is analysed using robust optimisation considering a high level of wind generation. Although robust optimisation has been applied to circumvent the challenges of uncertainty of wind and PV generators, the main disadvantage is that it only considers the worst case in the analysis of RES penetration level. The robust optimisation framework increases the operating cost that affects the optimal dispatch scheme. This is especially the case when a multi-objective optimisation problem is considered. It is generally unable to coordinate the multi-objective with a single min-max-min mathematical model [12].

In contrast to robust optimisation, the stochastic programming approach

uses a large number of scenarios to handle uncertainty in RES generation. In scenario generation method the stochastic variables are identified by the location, environmental parameters and renewable energy type. The analytical method includes fast Fourier transform method (FFTM), multi-linear simulation method (MLSM) and point estimation method (PEM) [13]. On the other hand, simulation methods such as Monte Carlo simulation (MCS) are used for PV and wind scenario generation, however, they are computationally inefficient compared to Latin hypercube sample (LHS). A two-stage stochastic DED is presented in [14], where the system variability is modelled in terms of uncertainty in wind generation and demand. The model is solved using a stochastic decomposition algorithm to take the uncertainty of wind generation and apply it to real-time applications. In [15], a stochastic unit commitment model is given for long-term generator allocation and dispatch which considers the uncertainty related to the load forecast errors and intermittent wind generation patterns. A multi-stage stochastic DED problem in [16] presents a multi-area transmission constrained problem. The uncertainty model is related to the multi-area RES production with the aim of increasing the dispatch storage. An integrated wind-thermal and energy storage self-scheduling model is demonstrated in [17] for energy and spinning reserve market. This study uses a three-stage stochastic framework to show the benefit of energy storage in the spinning reserve market. Authors in [18] presented a two-stage DED for a multi-wind farm generation considering copula correlation among the different wind farm sites. The solution is obtained by decoupling the stochastic variables and reformulating the problem as a deterministic DED. In [19], a dynamic carbon emission trading scheme is proposed for reducing carbon emission of thermal power generators by coordinating PV and wind generators in the energy mix to meet the Chinese carbon emission reduction targets.

A combined wind-thermal stochastic generation is presented in [20], from the utility's perspective. The model presented minimises the dispatch of thermal generators in each dispatch horizon while taking into consideration the uncertainty of wind generation and pool market. An optimal decomposition technique is utilised to solve the problem in real time. The uncertainties of wind generation and market electricity prices are modelled by a scenario generation approach. In [21], a stochastic scheduling DED model with multiple time resolution is presented for a high RES injection problem. The problem is presented in twofold, firstly a unit commitment problem is solved, and thereafter an economic dispatch model is solved for short term operations.

The literature reviewed shows that it is possible to integrate RES to the power system considering both the stochastic and robust optimisation framework while minimising RES curtailment. However, there is still a need for a detailed and optimal framework which considers renewable integration from the RO point of view. In this paper, we extend on the RO framework presented in [1] by introducing the stochastic nature of RES. This is done to quantify the level of RES generated daily while minimising the expected system operating costs. In addition, the proposed model aims to maximise the level of RES energy produced without the need for curtailment [22]. In this model, the scenarios for wind and PV output power are created to realise a RES quota from the SO perspective. The generation companies are subjected to penalties imposed by the SO, if they do not meet a minimum set out obligation. The battery energy storage system (BESS) is added to the model to leverage on the storage of excess energy from the RES to the BESS and it is only used in times of low-RES production and high demand. Moreover, it is also used to reduce the spinning reserves of the thermal generators. The contributions of this paper are listed below;

1. A novel stochastic multi-objective RO model is presented for joint scheduling of power dispatch and maximising RES penetration.
2. A stochastic multi-objective RO model is changed into a single objective function using weighting factor approach.
3. A preference-based approach is used to select an optimal solution from a Pareto Front set.
4. A BESS unit is introduced to support thermal generators in spinning reserve allocation.

The contents of this paper are organised into six sections. In Section 2 the RO policy framework is presented for the proposed stochastic model. In Section 3, the stochastic DED model is developed which includes PV, wind, BESS and conventional generators in the energy mix. In Section 4, a scenario generation method for wind and PV uncertainty is presented. Additionally, a scenario reduction method is presented and as well as a method for reducing redundant inactive constraints for a stochastic security constraint economic dispatch (SCED). In Section 5, the feasibility and efficiency of the proposed method are investigated on two test systems. Finally in Section 6 the conclusions are drawn.

2. Renewable obligation policy framework

The RO policy is focused on increasing the level of renewable energy in the overall electricity production. The fundamental premise behind any RO policy is to encourage investment in renewable energy by ensuring that renewable energy production is included in the electricity production portfolio of the country. Typically, the renewable target is set on an annual basis and increases gradually per annum. The generation companies have the choice of building their own RES as a strategy to achieve the RO target. Alternatively, they can also choose to buy ROC from third party companies. If they fall short of meeting the required RO, they are required to pay a penalty associated with the RES target deficit. This penalty is measured on every MWh of renewable energy produced. There are several technologies that are considered in the RO target, i.e., offshore wind and onshore wind, PV plant, tidal wave electricity generation, concentrated solar power generation, and geothermal generation. All the technologies have different ROC rating with the emerging technologies such as tidal energy having the highest ROC rating per MWh produced [23].

In the open market, where generation companies are competing against each other, RES can be at a disadvantage due to its inherent nature of variability and uncertainty associated with power production. The RO ensures that RES is included in the energy mix thus increasing the level of RES in the grid. The general framework proposed in this paper is such that the SO is responsible for optimal dispatching of all generators, and the RES generators are given first preference over thermal generators. Generation companies provide forecasts to the SO with a 1 day lead time. The SO is responsible for optimally scheduling the available power to meet the system demand. In addition, the SO also ensures the renewable target is attained daily by continuously monitoring the energy production and providing feedback to generation companies. A typical policy framework for the RO model is shown in Fig. 1.

In Fig. 1, the generation mix is made up of thermal, PV, wind, and BESS generating units. The policy framework is made up of three main components, i.e., the generation companies, the regulator or SO and the customers. The generators produce clean energy and the SO ensures that the renewable quota is achieved while maximising RES penetration and optimally scheduling energy and allocating the minimum spinning reserves.

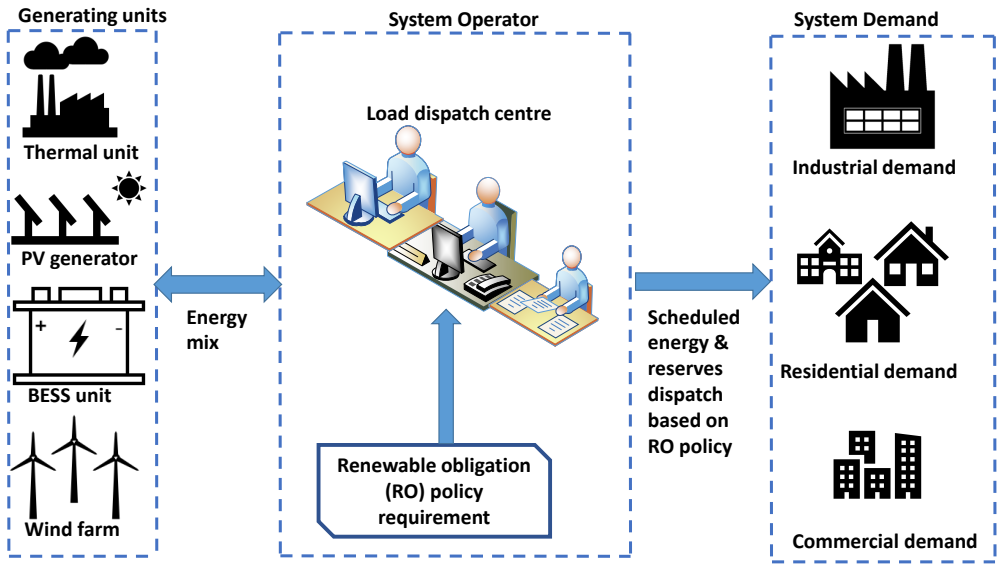

Figure 1: Renewable obligation policy framework for optimal energy mix and reserve allocation.

3. Problem formulation

The approach considered in this paper treats wind and solar power as non-dispatchable. The following assumptions are made for the formulation of the DED problem with RES obligation. All the RES (wind and solar) must be consumed first and the thermal generators must reduce their generation capacity to give preference to RES generators. The dispatch period considered in all the case studies is fifteen minutes. All RES are non-dispatchable and cannot be used as part of spinning reserves unless they have storage. The SO is responsible for dispatching all the generators including RES and BESS generators. The thermal and BESS generators can be used for spinning reserve. All the RES and BESS generators are owned by independent power producers (IPP).

3.1. Objective function

The objective is made up of two objective functions, i.e., the fuel cost minimisation with RO and the RES maximisation function. The objective

functions are as follows:

$$\min\ J_1 = \mathbb{E}\{C_T\} \tag{1}$$

$$\max\ J_2 = \mathbb{E}\{E_{RES}\} \tag{2}$$

3.1.1. Minimisation of the total operating cost C_T

The expected operating cost $\mathbb{E}\{C_T\}$ in (3) is made up of two terms. The first term is the total operating cost of each generating unit, that is, thermal generators, RES generators and BESS. For each scenario, the operating cost is multiplied by the probability of that scenario occuring. The second term is related to the RO policy framework which ensures an adequate energy mix.

$$\begin{aligned}\mathbb{E}\{C_T\} = \sum_{\omega=1}^{N_\Omega}\sum_{t=1}^{T}\pi_\omega\Bigg(\sum_{g=1}^{N_G}C_g(P_{g,t,\omega}) + \sum_{m=1}^{N_M}C_m(P_{m,t,\omega}) + \sum_{v=1}^{N_V}C_v(P_{v,t,\omega}) \\ + \sum_{s=1}^{N_S}C_s(P_{s,t,\omega}) + \sum_{r=1}^{N_R}C_{r,\omega}(P_{r,t,\omega})\Bigg) + \Gamma\end{aligned} \tag{3}$$

The second term of the RO model is presented by the notation Γ which is shown in (4).

$$\begin{aligned}\Gamma = \gamma\sum_{\omega=1}^{N_\Omega}\sum_{t=1}^{T}\pi_\omega\Bigg(\alpha\Bigg(\sum_{g=1}^{N_G}P_{g,t,\omega} + \sum_{m=1}^{N_M}P_{m,t,\omega} + \sum_{v=1}^{N_V}P_{v,t,\omega} + \sum_{s=1}^{N_S}P_{s,t,\omega}\Bigg) \\ - \Bigg(\sum_{m=1}^{N_M}P_{m,t,\omega} + \sum_{v=1}^{N_V}P_{v,t,\omega}\Bigg)\Bigg)^+\end{aligned} \tag{4}$$

The second term of the expression in (3) is the sigmoid function $\Gamma(\cdot)^+$ which is equal to γ if the renewable target is not achieved and 0 otherwise; α is the required RO in percentage which means that a portion of the total scheduled output power must come from RES. The penalty cost is represented by γ, which is the cost imposed for not achieving the RES obligation requirement and π_ω is the probability of each scenario. The generator cost function is a quadratic equation as shown in (5) where the units for the cost coefficients are $\$/MWh^2$, $\$/MWh$, and $\$/h$ and the generator spinning reserve cost is a linear function as shown in (6).

$$C_g\left(P_{g,t,\omega}\right) = \left(\frac{1}{n_0}\right)\sum_{g=1}^{N_G}\left(a_g + b_g P_{g,t,\omega} + c_g P_{g,t,\omega}^2\right) \tag{5}$$

$$C_r\left(P_{r,t,\omega}\right) = \rho_r P_{r,t,\omega}\Delta t \tag{6}$$

Note $n_0\Delta t = 1$ hour where $n_0 = 4$ and $\Delta t = 0.25$. This notation is introduced to ensure that the model can be applicable to any sampling period as long as it satisfies $n_0\Delta t = 1$ hour. The cost functions for wind and PV generators are shown in (7) [1] and (8) [24], respectively, and the operating cost for BESS generating unit is shown in (9) [25].

$$C_m\left(P_{m,t,\omega}\right) = \zeta_m P_{m,t,\omega}\Delta t. \tag{7}$$

$$C_v\left(P_{v,t,\omega}\right) = \varphi_v P_{v,t,\omega}\Delta t. \tag{8}$$

$$C_s\left(P_{s,t,\omega}\right) = \tau_s P_{s,t,\omega}\Delta t. \tag{9}$$

The costs of PV, wind and BESS comprise of a direct cost related to the SO buying energy from the IPP, where ζ_m is the wind energy cost in $\$/MWh$, φ_v is the PV energy cost in $\$/MWh$ and τ_s is the BESS energy cost in $\$/MWh$.

3.2. Maximisation of the renewable energy penetration

The second objective function is the maximisation of the expected renewable energy into the grid. It is worth noting that the second objective of the maximum renewable energy is partially covered by the minimisation of RO violation cost in the first objective function. If the renewable energy obligation can be met, then no penalty is imposed. The amount of renewable energy power scheduled to the grid may not be maximal. With the second objective function the amount of dispatched renewable energy has to be maximised to overcome the limitation of merely meeting the obligation without maximising the RES energy penetration. The second objective function is shown in (10).

$$\mathbb{E}\{E_{RES}\} = \sum_{\omega=1}^{N_\Omega}\sum_{t=1}^{T}\pi_\omega\left(\sum_{m=1}^{N_M}P_{m,t,\omega}\Delta t + \sum_{v=1}^{N_V}P_{v,t,\omega}\Delta t\right) \tag{10}$$

3.3. Constraints

The DED problem under investigation has five constraints which are considered as hard or soft constraints. These constraints are:

1) Real power balance which represents the sum of all generating units, i.e., the thermal generators, wind power generators and PV plant generators that should meet the forecast demand as given in (11).

$$\sum_{g=1}^{N_G} P_{g,t,\omega} + \sum_{m=1}^{N_M} P_{m,t,\omega} + \sum_{v=1}^{N_V} P_{v,t,\omega} + \sum_{s=1}^{N_S} P_{s,t,\omega} = \sum_{b=1}^{N_B} P_{b,t} \ \forall t, \forall \omega \tag{11}$$

The BESS stores excess energy and returns the energy back into the grid. In this paper, positive $P_{s,t,\omega}$ indicates the discharging mode and negative $P_{s,t,\omega}$ indicates the charging mode.

$$P_{s,t,\omega} = P^{d}_{s,t,\omega} x_{s,t,\omega} - P^{c}_{s,t,\omega} y_{s,t,\omega} \ \forall t, \forall \omega \tag{12}$$

where $P^{d}_{s,t,\omega}$ and $P^{c}_{s,t,\omega}$ are the discharging and charging power of the battery, and $x_{s,t,\omega}$ and $y_{s,t,\omega}$ are binary variables that ensure that discharging and charging do not take place at the same time as shown in (13) [26], [27].

$$x_{s,t,\omega} \mid y_{s,t,\omega} = \begin{cases} 1, & \text{if battery is charging;} \\ 0, & \text{if battery is discharging.} \end{cases} \tag{13}$$

2) Generator ramp rate and BESS stored energy. This is only applicable to thermal generators. The ramp up and ramp down units are in MW/h as given in (14).

$$P_{g,t,\omega} - P_{g,t-1,\omega} \leq UR_g \Delta t \ \forall g, \forall t, \forall \omega \tag{14a}$$
$$P_{g,t-1,\omega} - P_{g,t,\omega} \leq DR_g \Delta t \ \forall g, \forall t, \forall \omega \tag{14b}$$
$$P_{r,t,\omega} - P_{r,t-1,\omega} \leq UR_g \Delta t \ \forall r, \forall t, \forall \omega \tag{14c}$$
$$P_{r,t-1,\omega} - P_{r,t,\omega} \leq DR_g \Delta t \ \forall r, \forall t, \forall \omega \tag{14d}$$
$$E_{s,min} \leq E_{s,t,\omega} \leq E_{s,max} \ \forall t, \forall \omega \tag{14e}$$
$$E_{s,0,\omega} = E_{s,t_f,\omega} \ \forall t, \forall \omega \tag{14f}$$

3) Generator limits. The generator limits are applicable to thermal, RES and BESS generators. Equations (15) and (16), show the thermal generator

limits. Since $P_{m,t,\omega}$ and $P_{v,t,\omega}$ flow from wind and PV systems into the grid, respectively, they are represented by (17) and (18). The top limit is the forecasted wind power generation and solar power generation at time t, and scenarios ω, respectively. They both include the amount of power flow to the network and the remaining amount, which is either consumed locally or curtailed due to line capacity limit. The BESS limits are shown in (19) and (20). Equation (21), ensures that the charging and discharging of the battery cannot happen at the same time. The energy balance of the battery that considers the amount of charged or discharged energy and the relevant charging or discharging efficiency is given in (22).

$$P_{g,t,\omega} \leq min(P_{g,max}, P_{g,t-1,\omega} + UR_g) \ \forall t, \forall \omega \tag{15}$$
$$P_{g,t,\omega} \geq max(P_{g,min}, P_{g,t-1,\omega} - DR_g) \ \forall t, \forall \omega \tag{16}$$
$$P_{m,t,\omega} \leq P_{m,t,gen,\omega} \ \forall t, \forall \omega \tag{17}$$
$$P_{v,t,\omega} \leq P_{v,t,gen,\omega} \ \forall t, \forall \omega \tag{18}$$
$$0 \leq P^d_{s,t,\omega} \leq P^d_{s,max} \ \forall t, \forall \omega \tag{19}$$
$$0 \leq P^c_{s,t,\omega} \leq P^c_{s,max} \ \forall t, \forall \omega \tag{20}$$
$$x_{s,t,\omega} + y_{s,t,\omega} \leq 1 \ \forall t, \forall \omega \tag{21}$$
$$E_{s,t,\omega} = E_{s,t-1,\omega} - \frac{P^d_{s,t,\omega}\Delta t y_{s,t,\omega}}{\eta_d} + \eta_c P^c_{s,t,\omega}\Delta t x_{s,t,\omega} \tag{22}$$

4) Spinning reserve constraints.

$$P_{g,t,\omega} + P_{r,t,\omega} \leq P_{g,max} \ \forall g, \forall t, \forall \omega \tag{23}$$
$$0 \leq P_{r,t,\omega} \leq SRR_{r,max} \ \forall t, \forall \omega \tag{24}$$
$$\sum_{r=1}^{N_R} P_{r,t,\omega} \geq SSRR \ \forall t, \forall \omega \tag{25}$$
$$\sum_{g=1}^{N_G} P_{g,t,\omega} + \sum_{r=1}^{N_R} P_{r,t,\omega} + \sum_{s=1}^{N_S} P_{s,t,\omega} \geq \sum_{b=1}^{N_B} P_{b,t} \ \forall t, \forall \omega \tag{26}$$

where $P_{r,t,\omega}$ is the reserve contribution of unit g during time interval t and scenario ω. Constraint (24) represents the maximum reserve contribution for each generator where $SRR_{r,max}$ is the maximum contribution of unit g to the spinning reserve requirement (SRR). Constraint (25) is the minimum total system spinning reserve requirement (SSRR) for each time interval, and (26),

simply means that the sum of the total generation, spinning reserve and BESS generators must be able to support the demand without RES generators.

5) Network transmission constraints. For the economic dispatch problem, only the active power of the transmission line under RES forecast is considered as shown in (27).

$$-P_{l,max} \leq P_{l,t,\omega} \leq P_{l,max},\ \forall l, \forall t, \forall \omega \tag{27}$$

The transmission line power of line l at time interval t and scenario ω, which will be calculated by a nonlinear power flow for small size power systems, and DC power flow for large size power system is shown in (28), [28], [29].

$$P_{l,t,\omega} = \sum_{g=1}^{N_G} G_{l,g} P_{g,t,\omega} + \sum_{m=1}^{N_M} F_{l,m} P_{m,t,\omega} + \sum_{v=1}^{N_V} H_{l,v} P_{v,t,\omega} + \sum_{s=1}^{N_S} Q_{l,s} P_{s,t,\omega} - \sum_{b=1}^{N_B} D_{l,D} P_{b,t} \tag{28}$$

where $G_{l,g}$, $F_{l,m}$, $H_{l,v}$, $Q_{l,s}$ and $D_{l,D}$ denote the active power transfer coefficient factor between line l and thermal generator, wind farms, PV plant, BESS system and loads. The overall objective function is summarised as follows in (29).

$$\min\ J = (1 - \vartheta) J_1 - \vartheta J_2 \tag{29}$$

where ϑ is the weighting factor that converts the multi-objective functions into a single objective function, and a Pareto front is obtained by varying ϑ from 0 to 1. The objective function (29) is subject to constraints (11) - (28).

3.4. Formulation of multi-objective optimisation model

The proposed multi-objective optimisation model presented in the previous section is presented in its compact form as follows:

$$\min\ J(x) = \{J_1(x), J_2(x), \cdots, J_k(x)\}\ \forall k \in K \tag{30}$$

$$\text{s.t}\ h_i(x) = 0; \forall i \in N_I \tag{31}$$

$$g_j(x) \leq 0; \forall j \in N_J \tag{32}$$

where $J_1(x)$ to $J_k(x)$ represent multiple objective functions in (1) and (2), the value of K is 2, and x is the output vector which consists of an optimal dispatch solution for thermal and RES generators. The equality constraint in (11) is indicated by (31) and the inequality constraints from (14) to (28) is denoted by (32).

3.4.1. Pareto optimal solution

The multi-objective optimisation problem in (30) to (32), can be solved using the Pareto optimality principle. The optimal solution x^* in the feasible design space S is the Pareto optimal solution if and only if there exists no other point x in the set S such that $J(x) \leq J(x^*)$ with at least one $J_k(x) < J_k(x^*)$. The set of all Pareto optimal points refers to an optimal solution that is a compromise between the two objective functions. It follows that an efficient solution exists if a point x^* in the feasible design space S is efficient, and there is no other point x in the set S such that $J(x) \leq J(x^*)$ with at least one $J_k(x) < J_k(x^*)$. Otherwise, x^* is inefficient. Therefore, the set of all efficient points is called the efficient frontier. The Pareto optimal set is on the boundary of the feasible criterion space which also has a unique point called the Utopia point. A point J^0 in the criterion space is called the utopia point if $J_k^0 = min\{J_k(x)\}$ for all x in the set S [30], [31]. This point is obtained by minimising each objective function. Fig. 2, shows the Pareto fronts for bi-objective minimisation and maximisation problems.

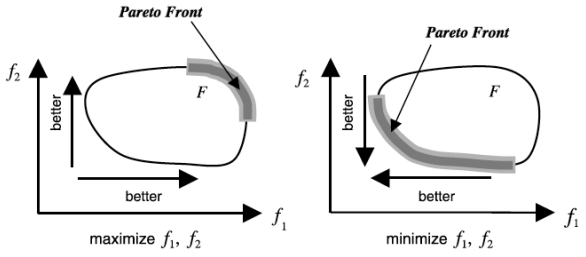

Figure 2: Pareto fronts for a bi-objective optimisation problem [32].

Fig. 2, also shows that the direction of the Pareto front depends on whether the bi-objective function is a maximisation or minimisation as illustrated by objective functions f_1 and f_2. The Pareto optimal solution demonstrates that there is no single dominant solution in the Pareto frontier but there is a set of solutions that can give an optimal solution. Moreover,

it is clear from the Pareto frontier that there is a trade-off associated with each Pareto point.

3.4.2. Normalising objective functions

As there are two objective functions that have different meanings and order of magnitude, it is important to normalise the objective functions to reduce the difficulty in comparison. It is usually necessary to transform the objective functions for all of them to have a similar order of magnitude. The objective functions are normalised as follows in (33).

$$J_k^{norm} = \frac{J_k(x) - J_k^0}{J_k^{max} - J_k^0}, \ \forall k \in K \tag{33}$$

where J_k^0 is the best point also known as the Utopia point of the objective functions and J_k^{max} are the worst point of the objective functions. The overall objective function J_k^{norm} will give values within the range of 0 and 1.

3.4.3. Weighted sum approach

In most practical engineering problems, there is a need for more than a single objective function to achieve all the system requirements. For example, in power system the SO always strives to achieve a trade-off between minimising the total operating cost and the expected emissions. There are generally two methods in the context of power systems that deal with multi-objective functions, namely, the ϵ-constraint and weighted sum method [33], [34]. A single objective function is considere in the ϵ-constraint method and the other objective functions are changed into constraints. These new constraints must satisfy a minimum ϵ value which measures the convergence of the optimisation model. On the contrary, the weighted sum method transforms all the objective functions into a single objective function by using weighting factors. The total sum of all the weights is equal to one. The main advantage of the weighted sum technique is the ability to provide efficient solution as opposed to the e-constraint which provides non-efficient solutions in linear problems. In this paper, a weighted sum technique is implemented to transform the multi-objective optimisation problem to a single objective problem. The weighting factor is varied from 0 to 1 to generate a Pareto front [1] as shown in (29).

3.4.4. Best compromise solution

There are different methods used in the literature that assist in selecting the best compromise solution. For example, in [35] a fuzzy set approach is

used to select the best solution by using a linear membership function. The membership function is assigned to the objective function which varies from 0 to 1 for measuring each Pareto optimal solution. In [36] a VIKOR technique is used for specifying the preferred solution and then ranking all Pareto solutions to the ideal solution. In this paper, a preference-based approach similar to [17] is used for the best compromise solution in a Pareto optimal set. To select the best compromise solution, the SO is the main decision maker. All decisions are implemented considering renewable obligation requirements, spinning reserve allocation, operating cost and RES penetration level. The SO determines the allowable values for both the total operating costs and the maximum RES penetration level. To this end, the SO selects the minimum lower bounds related to maximising RES penetration and upper limit for minimising the total operating cost. These upper and lower bounds assist the SO to select the best compromise solution on a Pareto optimal set.

4. Scenario generation for Wind and PV generators

The principles of these techniques are explained in the following subsections.

4.1. Scenario generation using Latin hypercube sampling

The generation power of PV and wind turbine depends on the environmental input. The variation of wind speed is a key factor for the evaluation of wind turbine output. As for the PV generation, the variation of solar irradiance is used to determine the output power of a PV plant. The uncertainty of wind power comes from the stochastic nature of wind speed while that of PV depends on external weather conditions such as clouds. The forecast errors of the RES generators are taken as random variables with specific PDF [37]. Afterwards, LHS method [32] is used to generate scenarios. The associated PV and wind power output scenarios are as follows.

$$P_{v,t,} = P_{v,t,f} + \Delta P_{v,t,e} \tag{34}$$

$$P_{m,t} = P_{m,t,f} + \Delta P_{m,t,e} \tag{35}$$

where $P_{v,t,f}$ and $P_{m,t,f}$ are forecasted value of the output wind and PV power and PV from the autoregressive moving average (ARMA) model and $P_{v,t,e}$

and $P_{m,t,e}$ are the prediction error of the output wind and PV power at time t which is defined by the ARMA(1,1) [38], [39].

$$\Delta P_{v,t,e} = \phi_v \Delta P_{v,t-1} + e_{v,t} + \theta_v e_{v,t-1} \tag{36}$$

$$\Delta P_{m,t,e} = \phi_m \Delta P_{m,t-1} + e_{m,t} + \theta_m e_{m,t-1} \tag{37}$$

where ϕ and θ are the auto-regressive and moving average parameters which are obtained by minimising the mean square error of the ARMA model from the historical data of RES output power. In this paper, the PDF of wind forecast error is considered as a Weibull distribution function. While a normal distribution function is used for the PV power forecast error. Moreover, for scenario generation purposes the empirical PDF and cumulative distribution function (CDF) from historical data are used. The RES data profiles are taken from [40] for a period of 2018.

The LHS method in [41], [42], is the method used to create scenarios of RES generation. Firstly, the PDF of the two uncertain variables are defined and their respective correlation matrix are created. LHS are used to generate different outcomes of dependent variables from different PDFs [43]. The following steps are employed to create 1000 scenarios of even probability.

1. Step 1: A Latin cube with the same number of independent variables is defined using the inverse cumulative distribution function (ICDF) of the normal variable with zero mean and a standard deviation of one to map the independent random variable of the sample to a value.
2. Step 2: The independent normal variables are formed from the Latin cube.
3. Step 3: The dependency to the independent normal variables is added using the Cholesky transformation which results in dependent variables. This means that when a normal CDF is applied to a normal random variable, the result is a uniform distribution between zero and one which still maintains the dependency between the variables.
4. Step 4: In the final step, the dependent uniform distributions are mapped using the ICDF to their original PDF, which results in dependent random variables.

4.2. Scenario reduction

In order to reduce the number scenarios, the initial scenarios are approximated by finite scenarios of even probabilities. The scenario reduction

determines a scenario subset and assigns new probabilities to the preserved scenarios so that the corresponding reduced probability measure is the closest to the original measure in terms of probability distance. The probability distance trades off scenario probabilities and distance of scenario values, and the Kantorovich distance of probability distribution is used for scenario reduction [44], [45]. The scenarios can be reduced using forward or backward reduction algorithm as described in [46]. The final reduced scenarios with their respective probability are used in the stochastic programming model as shown in Fig. 3.

4.3. Line capacity constraint reduction

The SCED increases the number of constraints based on the number of scenarios, number of transmission lines involved and the time horizon considered. Generally, the constraints increase when the problem is extended to the stochastic SCED model. Most security constraints are inactive and as a result do not affect the optimal solution. It is important to identify these inactive constraints; these can be eliminated to reduce the problem complexity. Authors in [47], identified an effective method of eliminating the inactive constraints without affecting the original optimal solution. The inactive constraints are only related to the system demand and transmission line parameters, and if the security constraint is inactive, then it is applicable as long as the system demand does not change.

Theorem 1 [47]. For a SCED optimisation problem with a feasible region $S = \{x \in R \mid Ax \leq b\}$, there exists a relaxed feasible region such that the kth constraint $A^k_{l,t,\omega}x \leq b^k$ is inactive and can be omitted in S and provided a new optimisation model $max\ A^k_{l,t,\omega}x \leq b^k$ is feasible if $A^k_{l,t,\omega} \leq P_{l,max}$.

A new problem is formulated as follows.

$$\begin{aligned} A^k_{l,t,\omega} = max\ & \sum_{g=1}^{N_G} G_{l,g}P_{g,t,\omega} + \sum_{m=1}^{N_M} F_{l,m}P_{m,t,\omega} \\ & + \sum_{v=1}^{N_V} H_{l,v}P_{v,t,\omega} + \sum_{s=1}^{N_S} Q_{l,s}P_{s,t,\omega} - \sum_{b=1}^{N_B} D_{l,D}P_{b,t} \end{aligned} \tag{38}$$

The objective function in (38) is subject to a power balance constraint (11) and generator limit constraints (15) to (21). The optimal solution is compared to the upper bound in (27) and if the optimal solution is smaller than

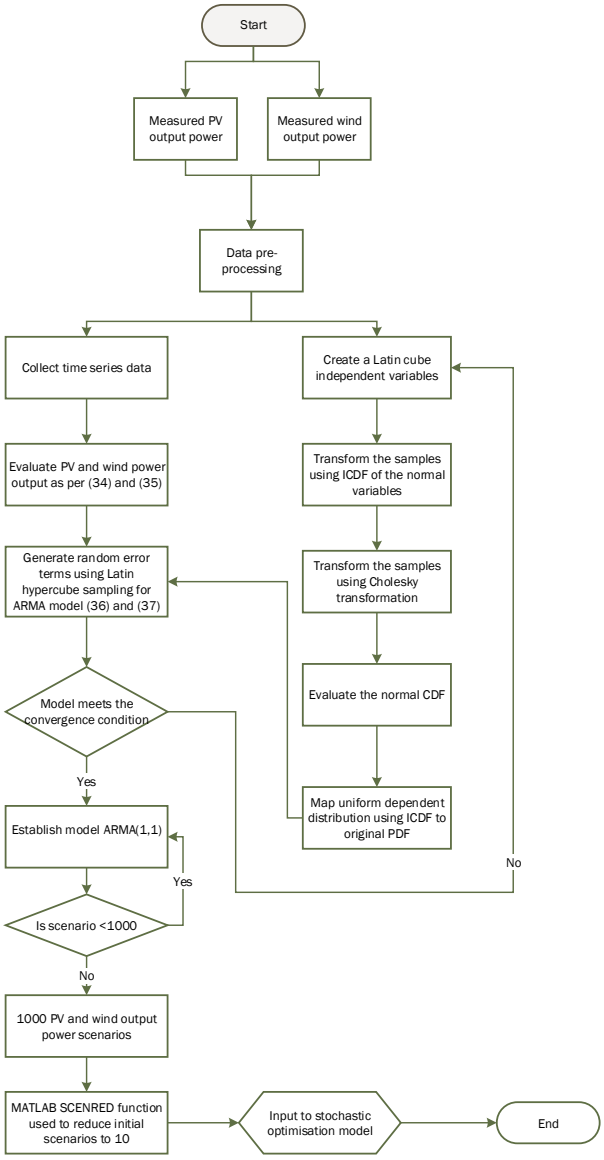

Figure 3: The process of generating scenarios from historical data using ARMA and LHS process to generate 1000 scenarios and then reducing the scenarios to 10 for stochastic optimisation model.

the upper bound, then the lth transmission line at time t and scenario ω is considered inactive and can be removed from the optimisation model [44].

5. Numerical case studies

The proposed optimisation model is applied to the IEEE bus test systems, i.e., the modified IEEE 30 and 118-bus systems. The historical data of RES generators and system load are obtained from Elia Group using a temporal resolution of 15-minutes [37]. The RES data is collected over a period of a year from January 1st 2018 to December 31st 2018. The integrated PV and wind farms are connected to buses 7, 15, 22, and 24. The modified IEEE 30-bus system has 6 thermal generators and 41 transmission lines. The ramp rates and quadratic cost coefficients are taken from [48]. The BESS system is connected to buses 26 and 28 respectively. The second IEEE 118-bus system, consists of 54 thermal generators and 186 transmission lines. Ten additional RES generators are added to the system on buses 1, 33, 38, 52, 68, 75, 96, 102 and 117. In the second test system, a combination of five PV and five wind systems is used. The BESS generators are added to buses 9 and 11. The details of the IEEE 118-bus system can be found in [49]. The fixed demand at each bus is the portion of the total capacity at each sampling period. The transmission line flow limit is simulated by using DC power flow and a sampling interval of 15 minutes is considered due to the intermittency of RES generators. The optimisation problem is solved over a 24-hour period. In the simulation studies, all the uncertainty is generated from 1000 scenarios which are further reduced to 10 scenarios and are solved using a deterministic approach. In all simulation studies, a RES penetration level of 10% is used as a benchmark and if the obligation is unattained, a penalty of $100,000 per day is imposed on generation companies by the SO. In addition, the system spinning reserves requirement is based on 30% of the maximum thermal generator capacity and the spinning reserves requirement of each generator is equal to the maximum generator capacity.

The optimisation problem presented in Section 3 is a mixed integer quadratic programming (MIQP) problem. The scenarios are generated and reduced using MATLAB [43], [45] and the optimisation model has been implemented using IBM ILOG CPLEX optimisation studio [50] on a quad-core 3 GHz desktop computer. The MIQP model is implemented by CPLEX using optimisation programming language (OPL). The main advantage of using CPLEX is the ease of software syntax to the mathematical representation of the op-

timisation problem. In order to show the effectiveness of the RO model the effects of the operating cost under RO target are analysed, the reduction in spinning reserve allocation due to BESS operating units and the impact of RES penetration on the overall energy mix. In all comparisons a RO target of 10% is used as a benchmark, and the RO model is tested on the IEEE 30-bus system to illustrate the effectiveness of the model by considering the following cases:

1. A comparison of the proposed stochastic RO model to the deterministic model to show the impact of RES intermittency on the key comparison parameters;
2. The impact of varying the RO target from 5% to 50% at a step of 5% on the overall energy mix and total operating cost;
3. The impact of using different penalty costs to measure the RES penetration level; and
4. The impact of changing the transfer limit on the overall RES penetration level.

Thereafter, IEEE 118-bus system is also used to test the model on a large scale test system to measure the effectiveness of the proposed stochastic RO model.

5.1. Implementation steps

The step-by-step approach for implementing the stochastic RO model for a combined energy and reserve dispatch is provided as follows.

1. Generate 1000 scenarios of wind and PV output power based on the scenario generation algorithm in Section 4.1.
2. Due to the high computation requirement for large scenario sets, the fast-forward reduction algorithm in [46] mentioned in Section 4.2 is applied to reduce the original 1000 scenarios to 10 scenarios.
3. Formulate the deterministic based joint energy and reserve scheduling under RO framework using the reduced scenarios as the input to the model.
4. Using the inactive constraint theorem presented in (38) the preliminary optimisation problem is solved, which reduces the number of inactive line capacity constraints that are related to the system demand and transmission line parameters.

5. Set the weighting factor in (29) to zero and solve the reformulated optimisation problem.
6. The reformulated MIQP is solved using dynamic search in CPLEX which is a search strategy for mixed integer programming (MIP) problems using the OPL parameter "MIPSEARCH".
7. Increase the weighting factor from 0 to 0.1 and solve the reformulated optimisation problem; iterate until the weighting factor is equal to 1.
8. Output the Pareto optimal set solution.
9. Applying the preference-based approach to select the best compromise solution using lower and upper boundaries of RES penetration and total operating costs.
10. Implement the best compromise solution and provide the optimal RO dispatch strategy.

The overall implementation flow chart is shown in Fig. 4.

5.2. Case study 1: IEEE 30-bus deterministic renewable obligation

In this section, the new model benefits are demonstrated by comparing the deterministic to the stochastic model. In order to compare the proposed model, the total operating cost, actual RES penetration level and the reduction in spinning reserves due to an increase in BESS penetration are used for comparison. The sizes of the PV plants are 500 MW and 275 MW and the size of the wind farms are 300 MW and 350 MW. The two BESS generators are rated at 15 MWh each and the charging and discharging efficiency is considered as 90%. The total installed capacities of RES and BESS generators are 1425 MW and 30 MWh, respectively. All the transmission line thermal limits are maintained at 100%. The IPP costs of energy for PV are 1.5 $/MWh and 3.0 $/MWh, and the costs of energy for wind are 1.3 $/MWh and 4.0 $/MWh and finally the costs for BESS are 1.36 $/MWh and 1.31 $/MWh, respectively [51]. Table 1 shows the thermal generator data. The daily forecasted demand and the power transfer thermal limit of each transmission line is shown in Fig. 5. The ARMA model for wind and PV output power is given in Table 2. All the fifteen minute data for demand and RES output power are obtained from EirGrid [40]. Figures 6 – 13, shows the RES output power for 1000 generated scenarios and the 10 reduced scenarios, respectively.

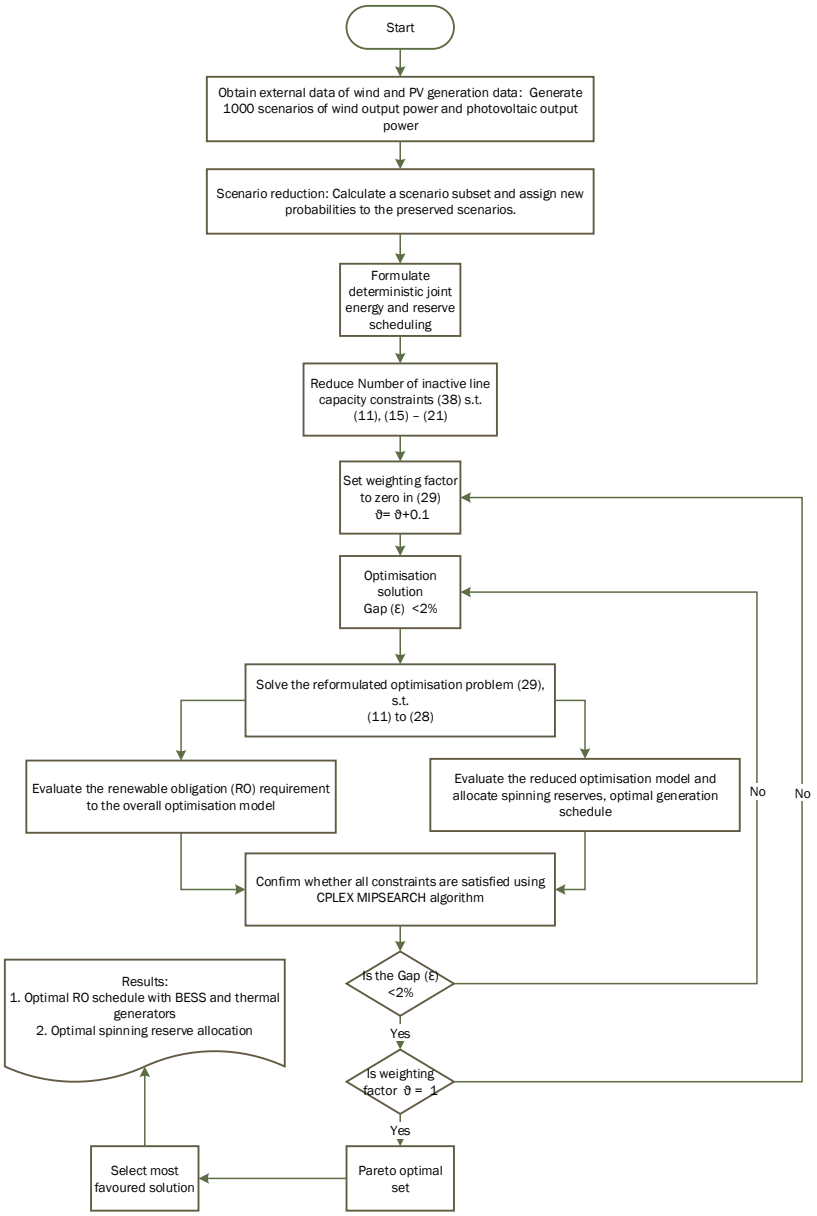

Figure 4: Optimisation algorithm for solving multi-objective stochastic RO model with Pareto optimal set and preference-based approach for selecting the best compromise solution.

Table 1: Thermal generator data.

Unit	Pmax	Pmin	a_g	b_g	c_g	RU	DR
G1	350	50	240	7.00	0.0070	60	60
G2	250	50	200	10.0	0.0095	60	60
G3	150	50	220	8.00	0.0090	60	60
G4	350	50	200	11.0	0.0090	60	60
G5	450	50	220	10.5	0.0080	60	60
G6	500	50	190	12.0	0.0075	60	60

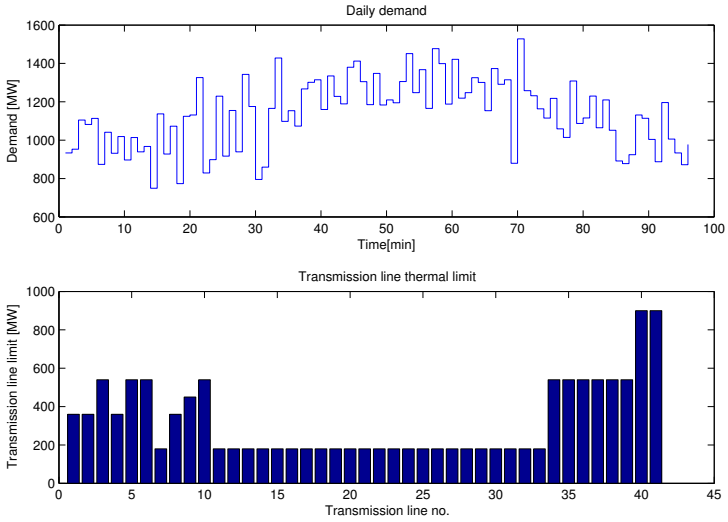

Figure 5: Forecasted demand and transmission line thermal limit for IEEE 30-bus system.

5.2.1. Solver parameter relaxation

A pre-solved relaxation parameter is used which performs the reduction with tight tolerances ($1e^{-10}$) than the default simplex tolerance ($1e^{-6}$) and offers more compact matrix and identifies obvious infeasibility much quicker. This is applied to the MIQP for root relaxation in order to perform preliminary reduction, elimination, substitution and coefficient modification in solving the optimisation model. Moreover, a dynamic search algorithm is used for solving a MIQP using a parallel mode switch parameter, and the continuous optimiser is set to solve the initial relaxation using dual simplex optimiser for root relaxation under the CPLEX OPL environment. The im-

Table 2: ARMA model for wind and PV output power.

Description	ϕ	θ
Wind 1	1.0	0.634012
Wind 2	0.968057	0.278895
PV 1	0.986552	-0.155482
PV 2	0.989746	0.072684

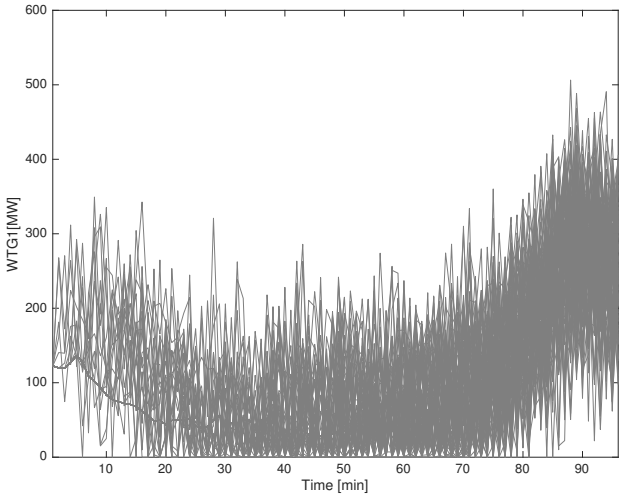

Figure 6: Forecasted wind power plant 1 with 1000 generated scenarios.

pact of implementing the relaxation parameter reduces the computing time and minimises the memory required to solve the optimisation model. Typically, the root relaxation computing time takes between 4 to 6 s while the overall root, branch and cut computing time is between 9 to 10 s compared to the default parameter setting which is between 30 to 60 s for the modified IEEE 30-bus system. In the MIQP model, a relative optimal solution gap parameter is set to 2%, which ensures that the relative tolerance on the gap between the best integer objective and the obtained objective falls below the 2% tolerance, this 2% error is good enough for the power dispatch purpose. When this tolerance is reached, the optimisation model terminates; however, under default settings, this parameter is set to 0.0001% which means that the optimisation model will continue the search until the relative solution

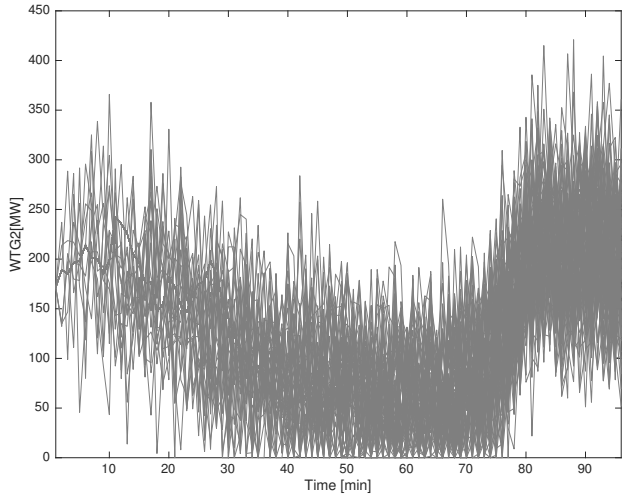

Figure 7: Forecasted wind power plant 2 with 1000 generated scenarios.

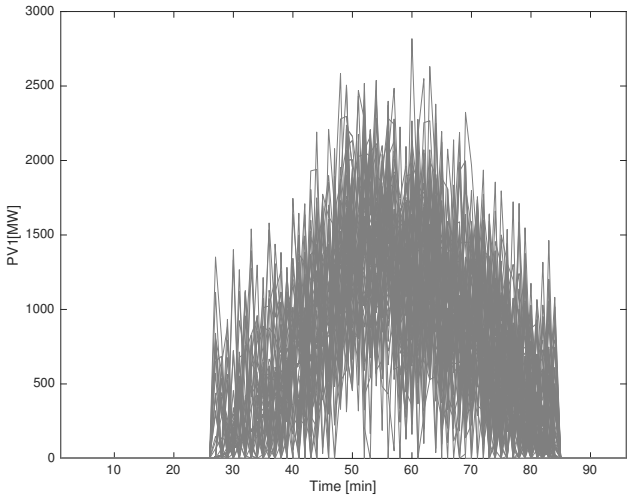

Figure 8: Forecasted PV plant 1 with 1000 generated scenarios.

gap falls below 0.0001%. The proposed parameter relaxation allows the optimisation model to reach an acceptable optimal solution much faster and saves memory compared to the default setting parameter.

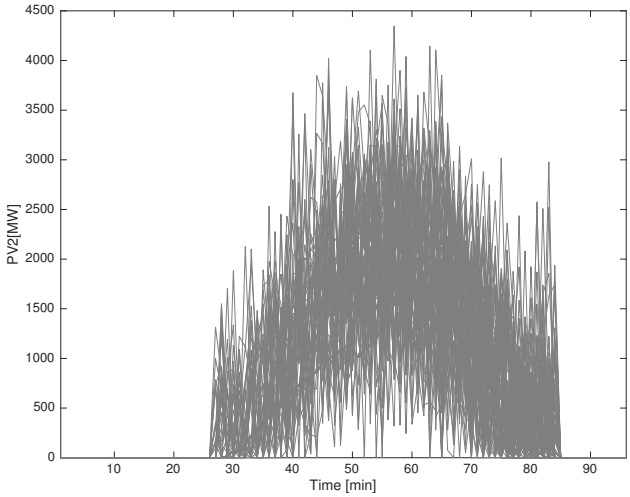

Figure 9: Forecasted PV plant 2 with 1000 generated scenarios.

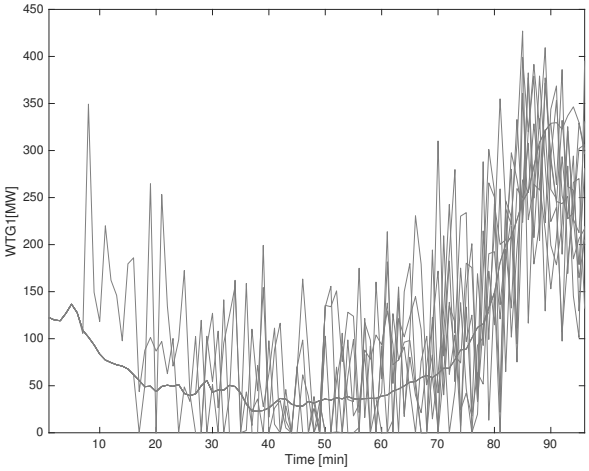

Figure 10: Forecasted wind power plant 1 with 10 scenarios.

5.2.2. Comparison of a stochastic and deterministic RES obligation model

In order to quantify the effectiveness of the proposed model, a benchmark base case simulation study is performed using the parameters in Table 1 and Table 2. The proposed model presented in Section 3, is compared to a

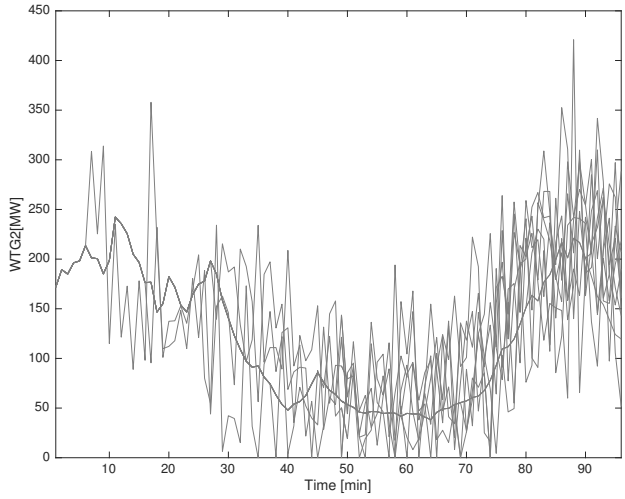

Figure 11: Forecasted wind power plant 2 with 10 scenarios.

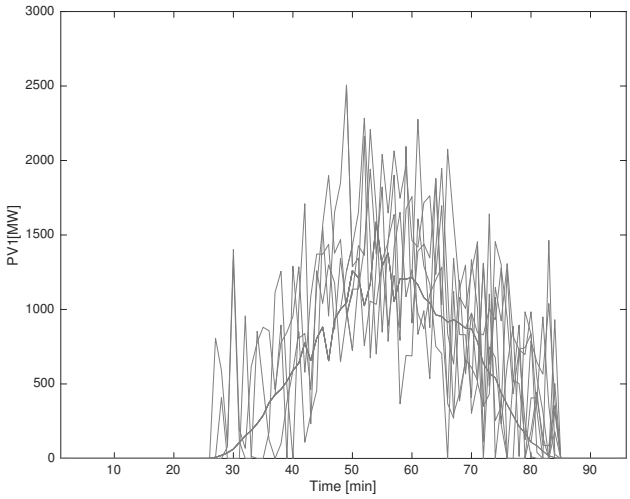

Figure 12: Forecasted PV power plant 1 with 10 scenarios.

deterministic version of the model. For the deterministic model, the total number of scenarios is equal to one which converts the stochastic model to a deterministic model. In both the deterministic and stochastic model the RO is set as 10%. A comparison in terms of the reduction in thermal energy

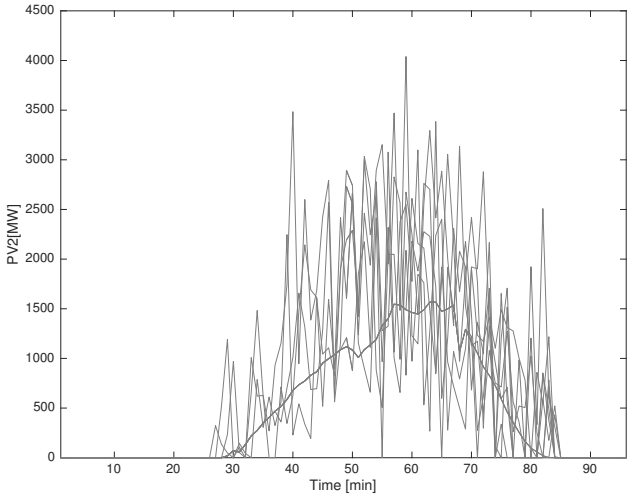

Figure 13: Forecasted PV power plant 2 with 10 scenarios.

production, an increase in RES production, a reduction in spinning reserve and an increase in battery storage due to excess RES production is provided in Table 3.

Table 3: Comparison between Pareto optimal solution and traditional DED.

	Stochastic			
Description	Best	Mean	Worst	Deterministic
Thermal (MWh)	58445	66125	76245	59144
PV (MWh)	31964	25894	17147	28954
Wind (MWh)	18890	17156	15533	20908
BESS (MWh)	-515	-391	-140	-222
SR (MWh)	50490	45432	35861	51885
RES (MWh)	50854	43050	32679	49865
RES (%)	46.74	39.57	30.04	45.84

A comparison of the deterministic to the stochastic model indicates that in both models, the RES obligation requirement is attained, with the deterministic achieving a maximum of 45.84% of RES penetration. For the stochastic model, the mean RES obligation is 39.57%. The best and worst

RES penetration levels are 46.74% and 30.04% respectively, which is above the RES obligation of 10%. There is an increase of 0.9% in RES penetration when a stochastic model is used. The stochastic solution presented in Table 3 corresponds to a single end point of the Pareto optimal solution when the RES energy is maximised and the total cost is minimised. Fig. 14 shows a comparison of the normalised Pareto front for the stochastic and deterministic model.

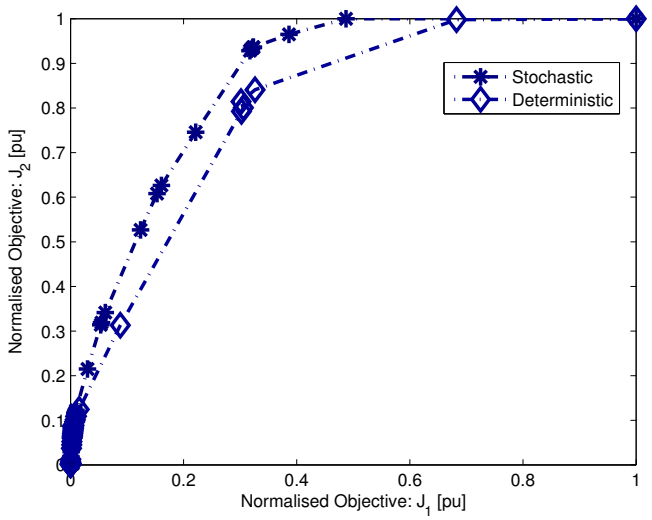

Figure 14: Comparison of stochastic and deterministic Pareto front.

The maximum and minimum operating cost for the stochastic model is \$829,910 and \$415,555 respectively while the total operating cost for the deterministic model is \$499,280 and \$320,030 respectively. When comparing the results shown in Table 3 between the stochastic and deterministic model, it can be inferred that modelling the intermittent nature of the RES generators increases the total operating cost whilst increasing the RES penetration and the required spinning reserves. The stochastic model increases the operating cost by 66% compared to a deterministic model. On the contrary, the stochastic model provides higher RES penetration and more precise solution for different scenarios. This means that solving a stochastic optimisation model provides better insight for the SO which provides the most likely scenarios in comparison to the deterministic approach.

5.2.3. The impact of renewable obligation requirement on the model sensitivity

In order to understand the impact of the RO parameter on the proposed model, the RO is varied from 5% to 50% at a step of 5%. This means the RES penetration level increases with each step change and the thermal and BESS system must increase their generation to support the demand while the spinning reserve will also increase with the increase in RES penetration. The Pareto frontiers for each RES obligation are shown in Fig. 15.

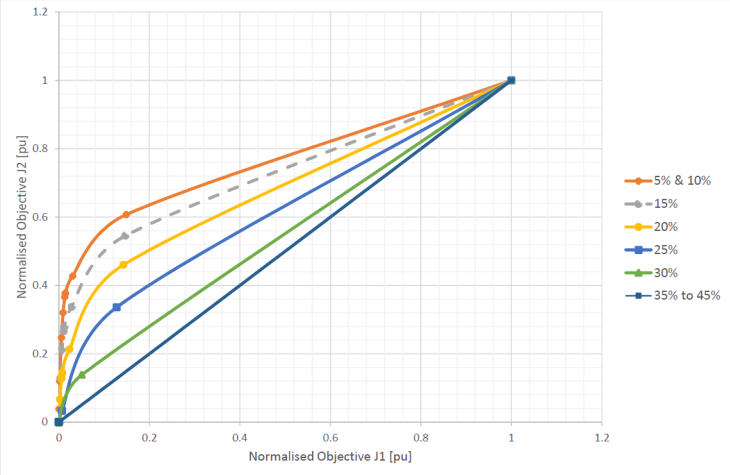

Figure 15: Pareto optimal solution for different RO target varying from 5% to 50%.

The impact of the RES obligation is variable. Fig. 15 shows the Pareto fronts for different RES penetration levels. The RES obligation is attained for a RES obligation of 5% to 45% and any RES obligation over 46% is unattained due to the transmission thermal limit. It is important to note that the Pareto front from 35% to 45% forms a Utopia line, which means that anything over 45% will result in a dominant solution that cannot be achieved and thus a penalty will be imposed. Fig. 16 indicates the average operating cost and RES penetration level for the stochastic model.

From Fig. 16 it is observed that the total operating cost increases with the increase in RES obligation requirement. The RES penetration level is achieved at all points except for when the obligation is set to 50%, which corresponds to the highest operating cost.

The impact of the weighting factor on the optimal solution is shown in Table 4. When the weighting factor is zero, the optimisation model in (29)

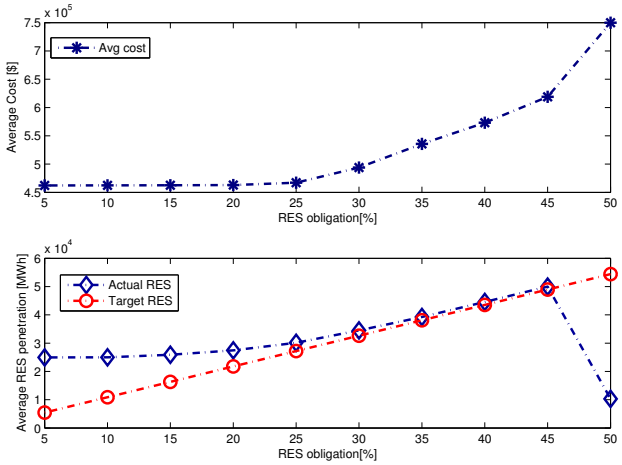

Figure 16: Expected average operating cost for different Pareto front and different RES penetration level.

changes into a minimisation of the expected operating cost which consists of thermal generating units, RES, BESS and spinning reserve allocation cost. The thermal generators produce more power, followed by wind and PV generators, and BESS units produce the least. The spinning reserve allocation respects constraint (25) which ensures that a minimum of 30% of the total production is always covered by thermal generators and BESS units. The maximum RES achieved is 46.75% which occurs when the weighting factor is 1. It can also be seen that for the maximum RES penetration scenario, excess RES energy is injected to the BESS units. This complies with the requirements of using BESS as a storage for excess RES energy injection as well as minimising spinning reserves from thermal generators. In this scenario, more spinning reserves are allocated from thermal generators than any other scenario. This implies that when RES is maximised, the SO must allocate more spinning reserves to overcome the intermittency nature of RES generators. If the end points are selected as the optimal solution to the multi-objective function problem, then the solution becomes bias as it only complies to a single requirement, i.e., the maximisation of the expected RES penetration or minimisation of the expected operating costs under RO. For example, the first end point provides the least expected operating cost with the least RES energy penetration, while the last end point gives a high RES energy penetration and high operating costs. An optimal solution must provide a

Table 4: Demand and supply for different weighting factor with the RO set to 10%.

ϑ	Gen (MWh)	RES (MWh)	SR (MW)	BESS (MWh)	TC ($)
0.00	97626.00	10878.00	32901.00	280.49	415560
0.10	96081.00	12422.00	32902.00	281.45	372851.8
0.20	92827.00	15672.00	32919.00	285.30	329881.6
0.30	87749.00	20754.00	32929.00	280.69	286331.8
0.40	84820.00	23696.00	32919.00	269.10	242215.6
0.50	83022.00	25500.00	32905.00	263.36	197720
0.60	82641.00	25905.00	32927.00	238.45	153021
0.70	82580.00	25976.00	32931.00	228.29	108278.8
0.80	80837.00	27971.00	34353.00	-23.92	63263.2
0.90	73819.00	35152.00	35137.00	-186.67	16080.2
1.00	58448.00	50860.00	50530.00	-523.51	-50860

compromise between minimising the expected operating cost and maximising the expected RES energy penetration. Based on the preference-based approach, the SO is the main decision marker. The SO can select the best compromise solution considering lower boundaries related to maximising RES penetration and upper boundaries for minimising the total operating cost.

Fig. 17 shows the Pareto front of the stochastic RO model when the RES quota is set to 10% with the optimal solution indicated by point A.

The lower and upper boundaries are selected as 30,000 MWh and $600,000. The Pareto optimal point provides a solution that realises a compromise in the expected operating cost and the expected RES penetration. The knee point shown as A in Fig. 17 corresponds to the weighting factor of 0.9 in Table 4. This point indicates a fair trade-off between minimising the expected operating costs while maximising the expected RES penetration in the grid and matches with the SO boundaries; any point away from the knee point will realise a non-compliant solution, in either direction. Although the minimum RES quota is achieved in the RO model the second objective function aims to maximise the expected RES penetration over and above the minimum RO requirement.

5.2.4. Importance of multi-objective functions

The RO model only focuses on setting a minimum quota in terms of renewable energy that must be achieved daily according to (3). The limitation

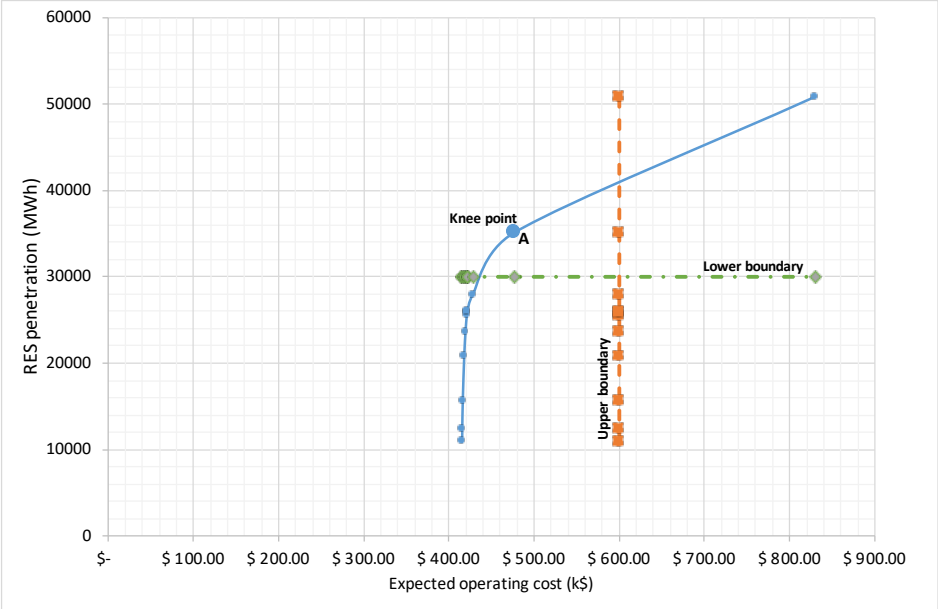

Figure 17: Pareto front optimal solution point 'A' with RO target set to 10%.

with the RO model is that it only aims to achieve the minimum stipulated RO and does not increase renewable energy over the stipulated quota, hence, there is a need to add an objective function that maximises the RES penetration. This function is shown in (2) and (10) as a RES energy objective function. It is important to note that although objective function achieves the RES obligation, it does not maximise the level of RES penetration. This is shown in Table 4, which indicates the Pareto optimal points for different weighting factors. For example, if a weighting factor of 0 is considered the operating cost is minimised and the RO is achieved, however, the RES is not maximised. When the weighting factor is increased gradually, the impact of objective function starts to increase the RES penetration over and above the RO quota in (3).

5.2.5. The impact of penalty cost on the model sensitivity

In this simulation study, the RES obligation penalty cost is varied in two steps, i.e., \$1000 and \$10,000 per day to quantify its impact on the RES penetration level which is varied from 10% to 20%. Fig. 18 illustrates the two RES penetration levels when penalty is varied. For example, when the RES

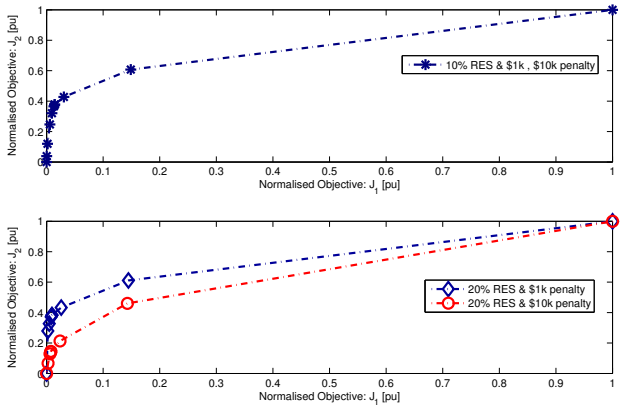

Figure 18: Average expected operating cost and RES penetration level.

obligation is 10% and the penalty is varied from \$1000 and \$10,000, the RES obligation is attained without any penalty. However, when the RES obligation is increased to 20% while varying the penalty, then the RES penetration is achieved only when the penalty is \$10,000 which results in an average RES penetration level of 27,463 MWh compared to 26,439 MWh of RES when the penalty is \$1000. The total operating costs for the two scenarios when RES obligation is 20% are \$462,862.7 and \$462,941.8, respectively for the \$1000 and \$10,000 penalty. The operating cost increases because in the first case when the penalty is \$1000, it is acceptable to not attain the RES obligation since the operating cost is minimal. The optimal solution presented shows that the proposed model is robust and can achieve RES penetration while considering the minimal operating cost for different RES obligation penalty cost.

5.2.6. The impact of transfer limits on RES penetration level

Initially, the transfer limits of the transmission line as shown in Fig. 5 are divided into five transfer limits which are 180 MW, 360 MW, 450 MW, 540 MW and 900 MW and the RES penetration achieved is 46.74%. In

order to show the effect of transfer limits on the RES penetration, two cases are considered; the transmission transfer limit is increased and decreased by 10% respectively. The optimal RES penetration level under different transfer limit is depicted in Fig. 19.

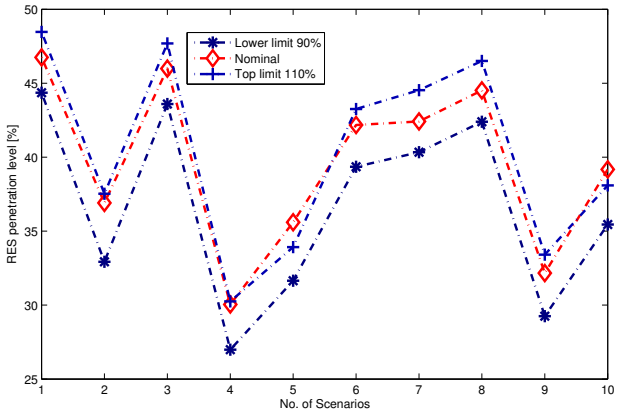

Figure 19: Impact of different transfer limits on RES penetration.

The impact of transmission limit is variable, which means that it may lead to an increase in total operating cost as well as the RES penetration when the limit is increased. However, when the limit is reduced, RES penetration level also decreases. This arises due to scheduling changes of the individual units. Specifically, the reduction in outputs of some units results in more RES penetration, while an increase in output of other units results in a decrease in RES penetration and spinning reserves as well as the total operating cost. The impact of increasing the transfer limit increases the operating cost and RES penetration level. On the other hand, the decrease in thermal limits leads to a decrease in total operating costs and RES penetration level.

5.3. Case study 2: IEEE 118-bus system

In the second case study, the proposed model is tested on a large-scale bus system. The system data for the IEEE 118-bus is from [49] and this system consists of 54 thermal generators and 186 transmission lines. The total thermal power installed is 12156 MW and the peak demand is 12147 MW. The sizes of the five wind farms are 250 MW, 1050 MW, 350 MW, 320 MW and 1600 MW, while the sizes of the five PV plants are 200 MW each.

The two BESS generators are rated at 35 and 40 MWh with the charging and discharging efficiency of 90%. The proposed model is used for calculating the total operating cost and RES penetration level.

5.3.1. Computational efficiency of the proposed model

This section explores the computational efficiency of the IEEE 118-bus system, due to the stochastic nature of the model presented in Section 3, there are generally many constraints that are inherent because of the number of scenarios. For example, the total number of line capacity constraints is the multiple of the time period (96), total number of transmission lines (186) and the number of scenarios (10). For the IEEE 118-bus system, the total number of transmission constraints is 357,120. When the inactive constraint reduction theorem presented in [47] is applied, the total number of inactive constraints is identified as 87%. The new transmission line constraints are reduced to 46,426 which reduces the solving time to 60 s.

In the first case the total number of line capacity constraints is considered and the time taken to solve the problem using parameter relaxation is 130 s compared to 60 s when the line constraints are reduced. In both cases, the RES obligation is attained and the total operating cost is \$4,500,900 with a standard deviation of 0.2%. From observations made, the computational efficiency shows that the proposed method can be utilised in scheduling RES, thermal and BESS units in a large-scale bus system.

5.3.2. Impact of RES obligation on model sensitivity

The impact of RES penetration on the model sensitivity is investigated in the IEEE 118-bus system. The total number of RES generators is increased from 4 to 10. The computed results are shown in Fig. 20 when varying the RES penetration from 10% to 50%. As can be seen in this figure, the total operating cost increases with the increase in RES penetration level. It is important to note that the total operating cost of the 30-bus system is considerably lower than that of the 118 bus system which is to be expected since the demand has increased and the network size is larger. The RES penetration level is achieved until 30% and any requirement over that results in a penalty. The reason for this limitation is due to the transfer limit on the transmission lines.

The average RES penetration achieved for the different obligation starting from 10% to 50% is 30.15%, 32%, 30.5%, 27.4% and 32.6% respectively. The highest operating cost occurs at 50% RES obligation which is \$4,645,909,

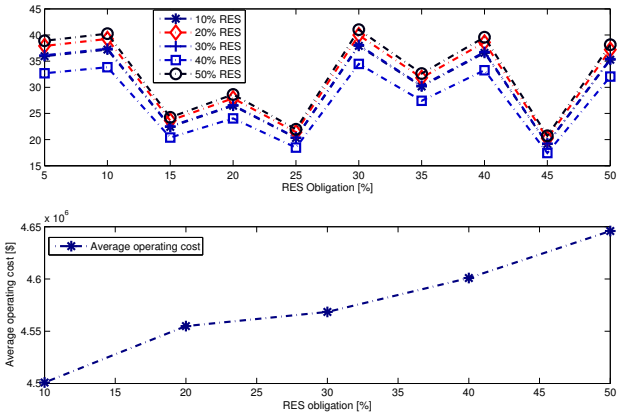

Figure 20: Average RES penetration and average operating cost for IEEE 118-bus system.

which corresponds to the RES penetration of 32.6% when the obligation is 50%.

5.3.3. Impact of BESS on spinning reserves and RES obligation

In this case study, 10 scenarios are considered for the evaluation of the proposed model. The achieved expected operating cost is $4,376,923.81 and the achieved maximum RES injection level is 34.47%, while the total reduction in spinning reserves is 0.19% and the BESS generation is -1132 MWh. This means that throughout the dispatch period the BESS is charging up with minimum discharge. It is clear that the stochastic model proposed is better in the approximation of the RES penetration level. Table 5 shows a comparison of the IEEE 118-bus generation for thermal, BESS, RES and the spinning reserves. The average operating cost achieved for the deterministic model is $4,017,379.10.

6. Conclusion

This paper proposes a stochastic economic dispatch model with renewable obligation requirement to maximise renewable energy penetration. The system operator is responsible for scheduling energy and spinning reserve under the renewable obligation framework. This framework aims to allocate the required renewable energy as part of an optimal energy mix strategy that reduces greenhouse gas emission. A dynamic scenario generation algorithm is

Table 5: Comparison of stochastic and deterministic RES penetration for IEEE 118-bus.

	Stochastic			
Description	Best	Mean	Worst	Deterministic
Thermal (MWh)	669433	741970	843566	790605
BESS (MWh)	-1132	-1874	-3095	-1272
SR (MWh)	370973	304732	208720	194101
RES (MWh)	352153	279979	178020	230981
RES (%)	34.47	29.83	17.43	22.61

used to characterise the intermittent nature of wind and photovoltaic output power and thereafter a scenario reduction algorithm is used in the renewable obligation model to schedule an optimal dispatch energy and allocate spinning reserves. To show the effectiveness of the proposed model, a 30-bus network with 6 thermal generators and 4 renewable energy sources is used to show the impact of high renewable energy penetration. Four cases were used to illustrate the effectiveness of the proposed renewable obligation model; in the first case a comparison of the deterministic and stochastic renewable obligation was performed based on the system operating costs, the reduction in spinning reserve allocation due to battery energy storage system and the achieved renewable energy penetration level. The comprehensive benefit of the four models were evaluated and thereafter we showed that the stochastic renewable obligation model is the most effective model in terms of the key measurement parameters. The sensitivity analysis was used to investigate other key parameters and the applicability of the proposed model. Our conclusion are as follows:

1. A benchmark renewable obligation target of 10% was used for the energy mix and output power of renewable energy sources was simulated using historical data. The simulated results show that higher renewable obligation can be achieved over and above the target.
2. The key indicator for any renewable obligation programme is the energy produced from renewable energy sources, which is used to issue renewable obligation certificates to all qualifying generation companies. The simulation studies show that it is possible to achieve high renewable penetration at a reasonable operating cost using the Pareto front approach.

3. A penalty is normally paid by generation companies for any renewable obligation shortfall; the simulation studies shows the different penalty factors used to validate the effectiveness of the proposed model and show the limitation and application in practical problems.
4. The maximum renewable penetration level is also limited by the available transmission thermal limits on the 30-bus network.
5. In a large 118-bus network, the computational effectiveness is improved by reducing the inactive transmission limit and a maximum of 87% inactive transmission constraints are reduced.

The current renewable obligation model does not take into consideration the trading of renewable obligation certificates. Therefore, the future research will include the risk associated with trading renewable obligation certificates in the secondary market.

Acknowledgements

The authors gratefully acknowledge the contributions of M. Sibiya, J. M. Singa, I. Bermejo Asensio and R. Gwandira for their work on the original version of this document. We are also grateful to the reviewers and editors for their valuable input. This work was supported in part by the South African National Energy Development Institute.

References

[1] T. G. Hlalele, R. M. Naidoo, J. Zhang, R. C. Bansal, Dynamic economic dispatch with maximal renewable penetration under renewable obligation, IEEE Access 8 (2020) 38794–38808.

[2] V. K. Jadoun, V. C. Pandey, N. Gupta, K. R. Naizi, A. Swarnkar, Integration of renewable energy sources in dynamic economic load dispatch problem using an improved fireworks algorithm, IET Renewable Power Generation 12 (9) (2018) 1004–1011.

[3] J. Yu, X. Shen, H. Sun, Economic dispatch for regional integrated energy system with district heating network under stochastic demand, IEEE Access 7 (2019) 46659–46667.

[4] V. Bassi, E. Pereira-Bonvallet, M. Abdullah, R. Palma-Behnke, Cycling impact assessment of renewable energy generation in the costs of conventional generators, Energies 11 (7) (2018) 1640.

[5] M. Hermans, K. Bruninx, E. Delarue, Impact of CCGT start-up flexibility and cycling costs toward renewables integration, IEEE Transactions on Sustainable Energy 9 (3) (2018) 1468–1476.

[6] Z. Cao, Y. Han, J. Wang, Q. Zhao, Two-stage energy generation schedule market rolling optimisation of highly wind power penetrated microgrids, International Journal of Electrical Power & Energy Systems 112 (2019) 12–27.

[7] M. M. Moarefdoost, A. J. Lamadrid, L. F. Zuluaga, A robust model for ramp-constrained economic dispatch problem with uncertain renewable energy, Energy Economics 56 (2016) 310–325.

[8] H. Zhang, D. Yue, X. Xie, Robust optimization for dynamic economic dispatch under wind uncertainty with different levels of uncertainty budget, IEEE Access 4 (2016) 7633–7644.

[9] A. Lorca, X. A. Sun, Adaptive robust optimization with dynamic uncertainty sets for mult-period economic dispatch under significant wind, IEEE Transactions on Power Systems 30 (4) (2015) 1702–1713.

[10] Y. Xu, M. Yin, Z. Y. Dong, R. Zhang, D. J. Hill, Y. Zhang, Robust dispatch of high wind power-penetrated power systems against transient instability, IEEE Transactions on Power Systems 33 (1) (2018) 174–186.

[11] L. Wang, B. Zhang, Q. Li, W. Song, G. Li, Robust distributed optimization for energy dispatch of multi-stakeholder multiple microgrids under uncertainty, Applied Energy 255 (2019) 113845.

[12] Z. Lin, H. Chen, Q. Wu, W. Li, M. Li, T. Ji, Mean-tracking model based stochastic economic dispatch for power systems with high penetration of wind power, Energy 193 (2020) 116826.

[13] S. Talari, M. Shafie-khah, G. J. Osório, J. Aghaei, J. P. Catalão, Stochastic modelling of renewable energy sources from operators' point-of-view: A survey, Renewable and Sustainable Energy Reviews 81 (2018) 1953–1965.

[14] Y. Liu, N. K. C. Nair, A two-stage stochastic dynamic economic dispatch model considering wind uncertainty, IEEE Transactions on Sustainable Energy 7 (2) (2016) 819–829.

[15] W. Lei, M. Shahidehpour, L. Tao, Stochastic security-constrained unit-commitment, IEEE Transactions on Power Systems 22 (2) (2007) 800–811.

[16] A. Papavasiliou, Y. Mou, L. Cambier, D. Scieur, Application of stochastic dual dynamic programming to the real-time dispatch of storage under renewable supply uncertainty, IEEE Transactions on Sustainable Energy 9 (2) (2018) 547–558.

[17] H. Khaloie, A. Abdollahi, M. Shafie-khah, A. Anvari-Moghaddam, S. Nojavan, P. Siano, J. P. Catalão, Coordinated wind-thermal-energy storage offering strategy in energy and spinning reserve markets using a multi-stage model, Applied Energy 259 (2020) 114168.

[18] M. Xie, J. Xiong, S. Ke, M. Liu, Two-stage compensation algorithm for dynamic economic dispatching considering copula correlation of multi-wind farms generation, IEEE Transactions on Sustainable Energy 8 (2) (2017) 763–771.

[19] Q. Tan, Y. Ding, Q. Ye, S. Mei, Y. Zhang, Y. Wei, Optimization and evaluation of a dispatch model for an integrated wind-photovoltaic-thermal power system based on dynamic carbon emissions trading, Applied Energy 253 (2019) 113598.

[20] A. Soroudi, A. Rabbie, A. Keane, Stochastic real-time scheduling of wind-thermal generation units in an electricity utility, IEEE Systems Journal 11 (3) (2017) 1622–1631.

[21] N. Li, K. W. Hedman, Economic assessment of energy storage in systems with high levels of renewable sources, IEEE Transactions on Sustainable Energy 6 (3) (2015) 1103–1111.

[22] S. Wang, B. Tarroja, L. S. Schell, B. Shaffer, S. Samuelsen, Prioritizing among the end uses of excess renewable energy for cost-effective greenhouse gas emission reductions, Applied Energy 235 (2019) 284–298.

[23] International Renewable Energy Agency, Renewable energy target setting (2015).
URL https://www.irena.org/documentdownloads/publications/irena_re_target_setting_2015.pdf

[24] M. Basu, Multi-region dynamic economic dispatch of solar–wind–hydro–thermal power system incorporating pumped hydro energy storage, Engineering Applications of Artificial Intelligence 86 (2019) 182–196.

[25] A. A. Eladl, A. A. ElDesouky, Optimal economic dispatch for multi heat-electric energy source power system, International Journal of Electrical Power & Energy Systems 110 (2019) 21–35.

[26] A. Kumar, N. K. Meena, A. R. Singh, Y. Deng, X. He, R. C. Bansal, P. Kumar, Strategic integration of battery energy storage systems with the provision of distributed ancillary services in active distribution systems, Applied Energy 253 (2019) 118–129.

[27] T. Adefarati, R. C. Bansal, Reliability, economic and environmental analysis of a microgrid system in the presence of renewable energy sources, Applied Energy 236 (2019) 1089–1114.

[28] X. Li, L. Fang, Z. Lu, J. Zhang, H. Zhao, A line flow Granular Computing approach for Economic dispatch with line constraints, IEEE Transactions on Power Systems 32 (6) (2017) 4832–4842.

[29] Y. Fu, M. Liu, L. Li, Multiobjective stochastic economic dispatch with variable wind generation using scenario-based decomposition and asynchronous block iteration, IEEE Transactions on Sustainable Energy 7 (1) (2016) 139–149.

[30] C. Roman, W. Rosehart, Evenly distributed pareto points in multi-objective optimal power flow, IEEE Transactions on Power Systems 26 (2) (2006) 1011–1012.

[31] J. Arora (Ed.), Introduction to optimum design, 4th Edition, Elsevier Academic Press, 2017.

[32] K. Lee, M. Al-Sharkawi (Eds.), Modern Heuristic Optimization Techniques: Therory and Applications to Power Systems, Vol. 39, John Wiley & Sons, 2018.

[33] R. Das, Y. Wang, G. Putrus, R. Kotter, M. Marzband, B. Herteleer, J. Warmerdam, Multi-objective techno-economic-environmental optimisation of electric vehicle for energy services, Applied Energy 257 (2020) 113965.

[34] P. Pourghasem, F. Sohrabi, M. Abapour, B. Mohammadi-Ivatloo, Stochastic multi-objective dynamic dispatch of renewable and CHP-based islanded microgrids, Electric Power Systems Research 173 (2019) 193–201.

[35] M. Shaterabadi, M. A. Jirdehi, Multi-objective stochastic programming energy management for integrated INVELOX turbines in microgrids: A new type of turbines, Renewable Energy 145 (2020) 2754–2769.

[36] A. Zakariazadeh, S. Jadid, P. Siano, Stochastic multi-objective operational planning of smart distribution systems considering demand response programs, Electric Power Systems Research 111 (2014) 156–168.

[37] M. N. Kabir, Y. Mishra, R. C. Bansal, Probabilistic load flow for distribution systems with uncertain PV generation, Applied Energy 163 (2016) 343–351.

[38] L. Ju, Q. Tan, R. Zhao, S. Gu, W. Wang, Multi-objective electrothermal coupling scheduling model for a hybrid energy system comprising wind power plant, conventional gas turbine, and regenerative electric boiler, considering uncertainty and demand response, Journal of Clearner Production 237 (2019) 1–16.

[39] J. M. Marales, A. Conejo, H. Madsen, P. Pinson, M. Zugno (Eds.), Integrating renewables in electricity markets, Springer, 2014.

[40] EirGrid. Grid data (2020). [link].
URL `http://www.elia.be/en/grid-data/data-download`

[41] S. Talari, M. Shafie-Khah, G. J. Osorio, J. Aghaei, J. P. S. Catalao, Stochastic modelling of renewable energy sources from operators‘ point

of view: A survey, Renewable and Sustainable Energy Reviews 81 (2) (2018) 1953–1965.

[42] M. Mazidi, A. Zakariazadeh, S. Jadid, P. Siano, Integrated scheduling of renewable generation and demand response programs in microgrids, Energy Conversion and Management 86 (2014) 1118–1127.

[43] Matlab., Latin hypercube sampling (2020).
URL https://www.mathworks.com/matlabcentral/fileexchange/56384-lhsgeneral-pd-correlation-n

[44] M. Zhang, X. Ai, J. Fang, W. Yao, W. Zuo, Z. Chen, J. Wen, A systematic approach for the joint dispatch of energy and reserve incorporating demand response, Applied Energy 230 (2018) 1279–1291.

[45] Matlab. Scenario reduction algorithm (2020). [link].
URL https://www.mathworks.com/matlabcentral/fileexchange?q=Scenred

[46] J. Dupacova, N. Growe-kuska, W. Romisch, Scenario reduction in stochastic programming: An approach using probability metrics, Math. Prog Series B 95 (3) (2003) 493–511.

[47] Q. Zhai, X. Guan, J. Cheng, H. Wu, Fast identification of inactive security constraints in SCUC problems, IEEE Transactions on Power Systems 25 (4) (2010) 1946–1954.

[48] F. Hu, K. J. Hughes, D. B. Ingham, L. Ma, M. Pourkashanian, Dynamic economic and emission dispatch model considering wind power under energy market reform A case study, International Journal on Electrical Power & Energy Systems 110 (2019) 184–196.

[49] IEEE, IEEE 118 Bus data (2020).
URL http://motor.ece.iit.edu/data/118bus_ro.xls

[50] IBM ILOG, CPLEX optimization studio (2020).
URL https://www.ibm.com/products/ilog-cplex-optimization-studio

[51] Eskom, Eskom Annual financial statements 31 March 2018 (Apr. 2020).
URL http://www.eskom.co.za/IR2018/Documents/Eskom2018AFS.pdf